Recent Progress in Ignition Fusion Research on the National Ignition Facility[*)]

Ramon J. LEEPER and The National Ignition Campaign Team

Sandia National Laboratories, Albuquerque, NM 87185 USA

(Received 17 December 2010 / Accepted 21 January 2011)

This paper will review the ignition fusion research program that is currently being carried out on the National Ignition Facility (NIF) located at Lawrence Livermore National Laboratory. This work is being conducted under the auspices of the National Ignition Campaign (NIC) that is a broad collaboration of national laboratories and universities that together have developed a detailed research plan whose goal is ignition in the laboratory. The paper will begin with a description of the NIF facility and associated experimental facilities. The paper will then focus on the ignition target and hohlraum designs that will be tested in the first ignition attempts on NIF. The next topic to be introduced will be a description of the diagnostic suite that has been developed for the initial ignition experiments on NIF. The paper will then describe the experimental results that were obtained in experiments conducted during the fall of 2009 on NIF. Finally, the paper will end with a description of the detailed experimental plans that have been developed for the first ignition campaign that will begin later this year.

Keywords: National Ignition Facility (NIF), National Ignition Campaign (NIC), Inertial Confinement Fusion (ICF) ignition, NIF diagnostics, NIF experimental plan

DOI: 10.1585/pfr.6.1104012

1. National Ignition Facility

The National Ignition Facility (NIF) located at the Lawrence Livermore National Laboratory is a 192-beam, 1.8-Megajoule, 500-Terawatt ultraviolet laser system that has a 10-m diameter target chamber with room for nearly 100 experimental diagnostics. NIF is the world's largest and most energetic laser experimental system providing a scientific center to study inertial confinement fusion (ICF) and matter at extreme energy densities and pressures. NIF is shown schematically in Fig. 1. NIF's laser architecture and laser sub-systems have been described in detail elsewhere [1–4]. Each of NIF's beams is a flashlamp-pumped neodymium-doped glass laser configured in a novel multi-pass master oscillator power amplifier (MOPA) system. The basic subsystems of NIF are the amplifier flashlamp power conditioning system, the injection laser system consisting of the master oscillator and high-gain preamplifier modules, the main laser system along with its optical components, the switchyards, and the target chamber and its experimental systems. The entire laser system, switchyards, and target area is housed in an environmentally controlled building. An integrated computer control system monitors, aligns, and operates the more than 60,000 control points required for NIF's operation. A large clean-room facility, the Optics Assembly Building, is located at one end of NIF for assembling and installing the precision optical and opto-mechanical components that make up the NIF laser system. On the opposite end of the facility the Diagnostics Building houses experimenters, data acquisition systems, and target preparation and storage areas. Over 3,000 46 cm × 8 cm × 4.1 cm glass slabs illuminated by 7,600 2 m long flashlamps comprise NIF's large amplifier systems. More than 7,500 meter-scale and 26,000 smaller optics are used in NIF for a total area of precision optical surfaces of nearly 4,000 m^2. These optics are assembled into thousands of precision cleaned and aligned line-replaceable units (LRUs) that form each beam line.

A key component in each laser beamline is a plasma-electrode Pockels cell (PEPC), utilizing potassium dihydrogen phosphate (KDP) plates, which acts as an optical

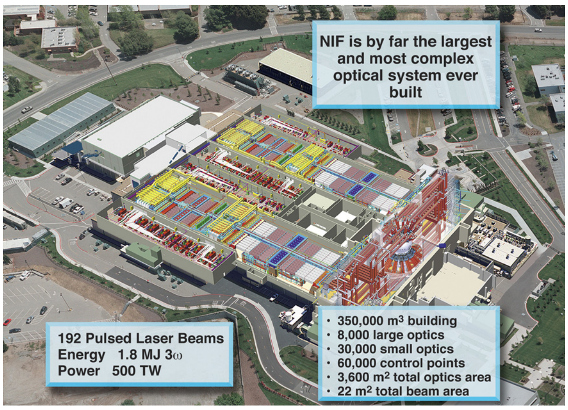

Fig. 1 Schematic of the NIF laser facility.

author's e-mail: rjleepe@sandia.gov

*) Sandia National Laboratories is a multi-program laboratory managed and operated by Sandia Corporation, a wholly owned subsidiary of Lockheed Martin Corporation, for the U.S. Department of Energy's National Nuclear Security Administration under contract DE-AC04-94AL85000.

switch. When combined with a polarizer, the PEPC allows light to pass through or reflect off the polarizer. The PEPC thus traps the laser light between two mirrors as it makes four one-way passes through the main amplifier system before being switched out to continue its way to the target chamber.

2. Indirect Drive Ignition Hohlraum and Target

The National Ignition Facility is designed to achieve fusion ignition in the laboratory using the inertial confinement fusion scheme. In the indirect-drive approach, the laser energy is converted to thermal x-rays inside a high Z cavity denoted as a hohlraum [5]. The x-rays, which bounce about inside the hohlraum, being absorbed and reemitted many times, are rather like light in a room where the walls are completely covered by mirrors. These x-rays then ablate the outer layers of a DT-filled capsule placed at the center of the hohlraum, causing the capsule to implode, compress and heat the DT and ignite. Note that the x-rays strike the capsule from all directions, smoothing out any irregularities in the incident NIF laser beams. Successful indirect drive ignition on the NIF requires driving the implosion capsule to high velocity (370 μm/ns) keeping the cryogenic deuterium-tritium fuel layer at low entropy. The imploded core must be round at stagnation to minimize cooling of the central hot spot by the adjacent cold, dense fuel. These three implosion requirements of high velocity, low entropy, and round shape are met by tailoring the radiation environment inside the laser-driven hohlraum. The multi-stepped radiation drive launches four shocks of precise timing (50-100 ps) and strength to minimize entropy addition to the cold fuel. The peak pulse of the drive accelerates the shell toward stagnation at the required velocity. Symmetric irradiation of the capsule is achieved by controlling the locations of the laser beam spots on the hohlraum walls and by adjusting the relative power deposited to the inner (equatorial) and outer (polar) spots [6].

The hohlraum must deliver the required drive and symmetry in the presence of laser-plasma interactions (LPIs) such as stimulated Raman backscatter (SRS), stimulated Brillouin backscatter (SBS), and crossed-beam interactions, which can reflect and redirect the laser light as it propagates through the hohlraum plasma. Reflection of laser light out of the hohlraum results in loss of x-ray drive on the capsule and potential loss of symmetry control. Redistribution of laser light inside the hohlraum via re-absorption of the reflected light also impacts symmetry control [5]. Michel et al. describe the physics of crossed-beam LPI in greater detail [7, 8].

The major features of the current NIF ignition target are shown in Fig. 2. The hohlraum is 5.44 mm in diameter and 10.01 mm long with two Laser Entrance Holes (LEH) that are 50-55% of the hohlraum diameter. The hohlraum

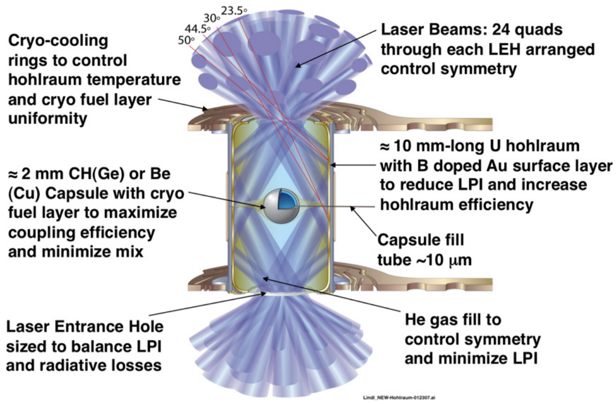

Fig. 2 Drawing of the NIF ignition hohlraum and capsule arrangement.

has Au-lined U walls and is filled with 0.9 mg/cm^3 of He tamping gas. Details of the LEH and other features of the target will be finalized to optimize performance based on the results of ongoing hohlraum energetics experiments that precede the capsule tuning experiments [6, 9]. To provide low mode symmetry, 24 sets of beams arranged in quads of 4 beams each enter from each side in sets of 4, 4, 8, and 8 at 23.5°, 30°, 44.5°, and 50°. The hohlraum is driven by a 1.3 MJ, 20 ns-long shaped pulse with 5 distinct phases: a 2 ns front picket to burn through the fill gas and set the initial shock, a 9 ns long trough to maintain a constant first shock velocity in the fuel, two further spikes to launch the second and third shocks, and a fourth rise to peak power for final acceleration of the shell at a peak radiation temperature T_{RAD} of 300 eV [10, 11].

The current design for the cryogenic capsule at hohlraum center is a graded Ge-doped CH ablator of 918 μm inside radius and 190 μm shell thickness enclosing a 68 μm-thick layer of solid DT fuel initially held near the triple point [12–15]. However, a variety of hohlraum and capsule options have been designed, spanning peak radiation temperatures between 270 and 310 eV and using either Cu-doped Be, Ge-doped CH or undoped or Mo-doped High Density (HDC) capsules [16–21]. Detailed sensitivity analyses for the current CH design are part of the preparations for the upcoming late 2010 campaign.

3. Radiation Hydrodynamics Codes

The NIF ignition hohlraum and target designs are performed with the ICF codes LASNEX and HYDRA. LASNEX is a two-dimensional (2D) axisymmetric radiation-hydrodynamics/multiphysics code [22]. HYDRA is a massively parallel three-dimensional (3D) radiation-hydrodynamics/multiphysics code that is used for very large 2D and 3D problems [23]. HYDRA has also been used for less-demanding 2D simulations, in much the same way as LASNEX.

Both codes are run with very similar physics models. For laser-driven hohlraums, in-line nonlocal-thermodynamic-equilibrium (NLTE) atomic physics model XSN to generate multigroup emissivity and opacity data for the gold and gold-boron hohlraum wall [24, 25]. The quotidian equation of state is used for hohlraum materials and gases at low temperature. At high temperatures, the XSN NLTE equation of state is used [26]. For capsule materials, more sophisticated LTE tabular opacities and equations of state are used.

4. Target Diagnostic System

The NIF diagnostic package contains an extensive suite of optical, x-ray, gamma ray, and neutron diagnostics that enable measurements of the performance of indirect driven NIF targets. A schematic of this system is shown in Fig. 3. Several review papers have been written on this topic that span a number of years [27–30]. The philosophy used in designing these diagnostics have emphasized redundant and independent measurement of fundamental physical quantities relevant to the operation of the NIF laser system, hohlraums, and ignition targets. A unique feature of these diagnostics is that they are being designed to be capable of operating in the high radiation, electromagnetic pulse, and debris backgrounds that are generated in NIF experiments. The NIF diagnostic system can be categorized into three broad areas: laser characterization, hohlraum characterization, and capsule performance diagnostics.

The laser power incident on the hohlraum is measured using NIF's laser diagnostics: The power delivered by each quad is measured with ±3% accuracy by a combination of fast diodes and calorimeters in the $1\,\omega$ (1053 nm) and $3\,\omega$ (351 nm) sections of the laser. The NIF laser beams are smoothed by continuous phase plates smoothing by spectral dispersion (SSD), and polarization smoothing (PS). Two static x-ray imager (SXI) pinhole cameras image the laser-entrance holes of the hohlraum at a polar angle of 19° to the hohlraum and target chamber axis [31].

The backscattered power reflected out of the hohlraum

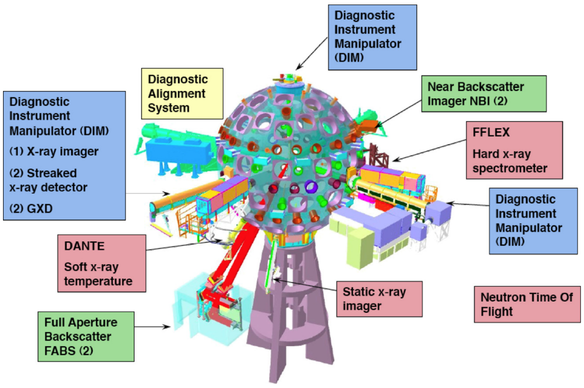

Fig. 3 Shown here is a schematic of the NIF diagnostic system.

is measured directly on one 30° inner-cone quad and on one 50° outer cone quad by a pair of diagnostic systems. The full-aperture backscatter station (FABS) measures the energy, power, and spectrum of the SRS and SBS light reflected back into each of the four f/20 final optics apertures in a quad [32]. The near backscatter imager (NBI) measures light scattered within a ≈ f/4 cone around the quad center [33]. Together with a pulsed-laser calibration system, they are capable of measuring the backscattered quad on each of the diagnostic quads with ±15%-20% accuracy.

An important hohlraum diagnostic is the broadband soft x-ray spectrometer DANTE that measures the x-ray flux and spectrum emitted from the laser-entrance holes at an angle of 37.5° to the hohlraum axis. DANTE is an absolutely calibrated, 18-channel filtered x-ray diode array that measures x-rays with photon energies ranging from 70 eV to 10 keV [34]. Using the response function of each channel, the x-ray spectrum emitted by the hohlraum can be unfolded as a function of time [35, 36]. Another important hohlraum energetics diagnostic is the filter-fluorescer array FFLEX. FFLEX measures the hard x-rays >20 keV generated by hot electrons. The FFLEX data are unfolded by assuming a two-temperature bremsstrahlung spectrum to produce a hot electron energy and characteristic temperature $E_{\rm hot}$ and $T_{\rm hot}$ [37].

Hohlraum symmetry tuning uses the gated x-ray detector (GXD), a filtered x-ray pinhole snout mounted in front of a micro-channel plate-phosphor-charge coupled device camera stack [38]. The GXD takes four 200 ps long time records of the imploding capsule self-emission. The GXD is pointed in the equatorial plane of the hohlraum, i.e., it views the capsule from the side of the hohlraum. The shape of the imploded core self-emission is a sensitive measure of the laser power distribution inside the hohlraum. The time of each diagnostic record is referenced to the start of the NIF laser pulse using the NIF cross-timing system. This enables the GXD, in addition to measuring the shape of the imploded core, to measure the time of peak x-ray brightness, or "bang time", to an accuracy of ±50 ps.

A large number of nuclear diagnostic techniques are being developed for NIF. These include nuclear activation methods, neutron time-of-flight techniques, wedge range filter methods, neutron imaging, magnetic recoil spectrometer, fusion reaction history, tertiary neutron and proton spectroscopy, and proton radiography [27–30, 39–49].

5. NIC Experimental Plans Leading Up To Ignition

The NIC experimental plans are structured to validate the NIF Ignition Point Design target. Four integrated teams are developing the requirements for the campaigns leading up to ignition. The first of the teams is focused on laser performance and is defining the requirements for pulse shaping, power balance, pointing, and beam conditioning. The second team is focused on hohlraum performance and is considering the requirements in the area of hohlraum energy coupling, hohlraum radiation characteristics, radiation symmetry, and x-ray and electron preheat. The third team is focused on capsule performance and is defining the requirements on shock timing, ablator physics, and hydrodynamic stability. The fourth team is focused on the ignition experiments and is defining the overall ignition campaign plan, integrated implosions, and ignition diagnostics.

During the fall of 2009, the first NIC hohlraum energetics experiments were conducted using all of NIF's 192 beams incident onto 82%-scale hohlraums operated at laser energies of 520 kJ and 700 kJ [6, 9]. This scale of hohlraum operated at 520 kJ has close to the same hohlraum performance and internal plasma conditions as that of a 1.2 MJ, 285 eV radiation temperature full-scale ignition hohlraum. When this scale hohlraum is operated at 700 kJ, its hohlraum performance and internal plasma conditions are close to those of a 1.4 MJ, 300 eV radiation temperature full ignition hohlraum. The results of these hohlraum energetic experiments indicate that the NIC program is on a path to a $T_{\mathrm{RAD}} = 300$ eV ignition hohlraum design that uses 1.2-1.5 MJ of laser energy. These experiments demonstrated reduction of SRS backscatter losses by filling the hohlraum with pure helium rather than a hydrogen/helium originally thought optimal in early NIF ignition target designs. Total backscatter levels are below 10% for helium-filled hohlraums with outer cone backscatter $\delta \leq 2\%$. The experiments also demonstrated that the hot electron fraction $f_{\mathrm{hot}} = E_{\mathrm{hot}}/E_{\mathrm{laser}}$ is below 2% on all shots. Keeping the hot electron fraction low is important because of its effect on raising a capsule's entropy and its effect on shock velocity [50, 51]. The experiments showed that peak x-ray flux measurements are close to ICF design code descriptions and that calculations using the point-design model are conservative with respect to x-ray drive. X-ray bang time data show that capsule velocity varies with hohlraum radiation temperature as predicted by the design codes, although the offset between measured and calculated bang times must be investigated further. Together, these results point toward 1.2-1.5 MJ hohlraums that can meet ignition specifications at $T_{\mathrm{RAD}} = 300$ eV. Further, vacuum hohlraum experiments conducted on NIF have demonstrated increased x-ray conversion that is attributed to the increased volume-to-surface area of the larger NIF hohlraums [52].

An ignition tuning campaign will empirically correct for residual uncertainties in the implosion and hohlraum physics used in the NIF radiation-hydrodynamic computational models before proceeding to cryogenic-layered implosions and ignition attempts [10, 11]. This will be accomplished using a variety of surrogate targets that will set key laser, hohlraum, and capsule parameters to maximize ignition capsule implosion velocity, while minimizing fuel entropy, core shape asymmetry and ablator-fuel mix. This is followed by intentionally "dudded" tritium-rich but deuterium-poor cryogenic-layered implosions to check the efficacy of the tuning through shared observables such as core symmetry and bang time and from implosion performance. Finally, if the chosen ignition design called for larger scale, the tuning would be checked at this larger scale, before proceeding to tests of alpha heating and ignition.

Ignition requires a pulse shape with a low power foot designed to send a carefully timed series of four shocks through the frozen DT shell such that they overtake each other soon after they travel into the enclosed DT gas. If the shocks are too closely spaced, they will coalesce within the DT ice leading to an increase in the entropy at the inside surface of the DT ice, reducing compressibility. If they are too widely spaced, the DT ice decompresses between shocks. Since radiographic methods of assessing shock front velocities to the required 1%-2% accuracy would require unrealistic sub micrometer accuracy after accounting for the fuel compression that occurs after each shock passage, a direct continuous measurement of the shock velocity technique has been adopted for these measurements. This is achieved by reflecting off the shock front using a streaked 1D imaging laser-based velocity interferometry system "VISAR" from which shock front velocities are extracted with the required 2%-5% accuracy from fringe shifts and overtake distances extracted by integrating the velocity between time of first shock breakout from the ablator-fuel interface and time of the next shock overtake seen as a sudden jump in fringe shift. A schematic of the experimental arrangement that will be used in timing the first three shocks on the NIF ignition target is shown in Fig. 4 [10, 11, 53].

As for the second and third shocks, a correctly timed fourth shock (overtaking the first three shocks only after they have coalesced to ±100 ps timing) is critical for keeping the fuel adiabat low for maximum compressibility [10, 11, 54]. Too early a fourth shock will lead to fourth shock overtake in the fuel and an increase in entropy. In ad-

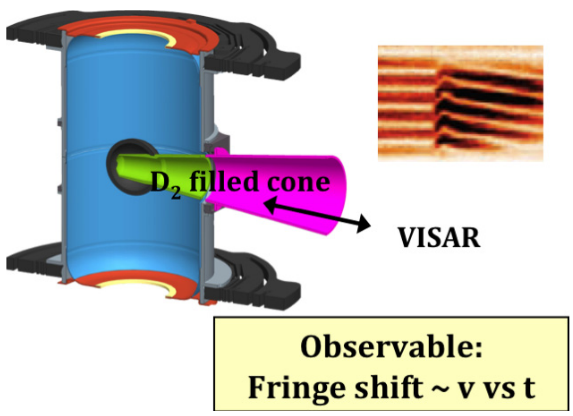

Fig. 4 Experimental geometry for timing the first three shocks of the NIF ignition target.

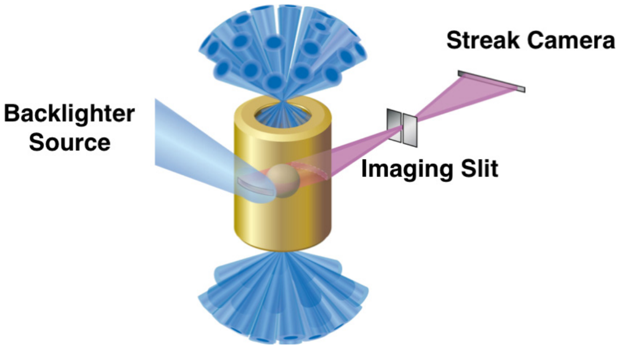

Fig. 5 Shown here is a schematic of the experimental setup that is used to measure ablator mass and velocity from a single, streaked radiograph.

dition, too fast a fourth rise at any launch time leads to too strong a fourth shock and increased entropy. Finally, too late or long a fourth rise delays the onset of peak power and leads to poorer coupling of the main drive to the capsule since its surface area is continually shrinking after the first three shocks' passage, resulting in reduced implosion velocity at fixed peak power.

Due to the VISAR window blanking at peak hohlraum drive levels, fourth pulse timing and strength has to be tuned from observing shock breakout time through an opaque witness plate combined with a soft x-ray measurement of the fourth pulse rise of the hohlraum drive [54].

For a given ignition design characterized by a peak laser power and laser energy, choice of hohlraum and capsule type and size, and initial assumptions on hohlraum and capsule coupling efficiency, there is an optimum setting for the combination of peak implosion velocity and amount of ablator mass remaining at implosion stagnation. An initially thin capsule can be driven to high implosion velocity in 1D, but per the rocket equation, that leads to little residual ablator mass remaining, hence enhanced feed through of Rayleigh-Taylor instability growth and eventually to DT fuel preheating by x-rays. An initially thicker capsule will be more immune to shell breakup by hydro instabilities, but reach insufficient peak implosion velocity to provide enough *PdV* work to ignite the hotspot.

The approach to NIC ablator tuning is by streaked or gated x-ray radiography that will extract through Abel inversion the time-resolved ablator density profile from which remaining mass, areal density, position, and velocity of the ablator as a function of time can all be derived [10, 11, 55, 56]. The experimental setup for this measurement is shown in Fig. 5. The capsule is identical to the ignition capsule except for the 70 μm of DT ice replaced by an equivalent areal density of Be, 10-μm-thick to maintain fidelity in its trajectory. The radiography source is an area backlighter in transmission mode created using two 50-degree quads irradiating a 5-7-μm-thick backlighter foil (Ni He-alpha 7.8 keV for the BeCu design, Cu He-alpha 8.4 keV for the CH (Ge) and HDC designs) placed on the side of the hohlraum. 125-μm tall by 1.5-mm-long slots are cut out of the hohlraum wall opposite each other to allow a fan of x-rays to backlight the capsule equator. They will be filled and encased in several 100 μms of HDC to delay slot closure.

The symmetry capsule became a robust technique for tuning both vacuum and gas-filled hohlraums in Nova hohlraums, where changing hohlraum length and/or beam pointing set the time-averaged single beam cone location near the P_2 node [3, 10, 11]. At OMEGA, the NIC concept of setting symmetry by balancing opposite sign P_2 from different beam cones was first demonstrated followed by rudimentary beam cone phasing. The technique has been successfully ported to NIF in recent 500 kJ symmetry experiments [10, 11].

A capsule performance optimization campaign will experimentally correct for residual uncertainties in the implosion and hohlraum physics used in our radiation-hydrodynamic computational models before proceeding to cryogenic-layered implosions and ignition attempts. As described above, the required tuning techniques for shock timing, ablator mass remaining, and symmetry have been shown experimentally and computationally to meet the required sensitivity and accuracy. The first cryogenic-layered implosions will employ capsules filled with tritium, hydrogen, and a small fraction of deuterium (~ 2-10%). These so called THD capsules are designed to be hydrodynamically equivalent to DT capsules filled with 50% D and T [57]. These capsules have the advantage of keeping the neutron yield low and allow the full complement of optical, x-ray, and gamma-ray diagnostics to be employed in these experiments in addition to nuclear diagnostics. An important measurement during these THD experiments is the ρR from down-scattered neutrons using the neutron time-of-flight diagnostic and the magnetic recoil spectrometer diagnostic [39, 44]. The THD shots will be followed by full DT ignition shots [57].

6. Summary

It is a truly exciting time to be a part of the NIC team. NIF is now up and fully operational as the world's largest and most energetic laser experimental system that will enable the first ever attempt at ignition in the laboratory.

Acknowledgements

We would like to acknowledge the help we have received in assembling these lecture notes from B.J. MacGowan, M.J. Edwards, S.H. Glenzer, O.L. Landen, N.B. Meezan, E.I. Moses, and R.E. Olson through personal conversations as well as from their published and unpublished papers.

[1] E. Moses *et al.*, Fusion Sci. Technol. **43**, 420 (2003).
[2] M.A. Lane and C.R. Wuest, eds., Proc. SPIE, Vol.**5341**

(2004).
[3] G.H. Miller, E.I. Moses and C.R. Wuest, Nucl. Fusion **44**, S228 (2004).
[4] E. Moses and C.R. Wuest, Fusion Sci. Technol. **47**, 314 (2005).
[5] J. Lindl *et al.*, Phys. Plasmas **11**, 339 (2004).
[6] N.B. Meezan *et al.*, Phys. Plasmas **17**, 056304 (2010).
[7] P. Michel *et al.*, Phys. Rev. Lett. **102**, 025004 (2009).
[8] P. Michel *et al.*, Phys. Plasmas **17**, 056305 (2010).
[9] S.H. Glenzer *et al.*, Science **327**, 1225 (2010).
[10] O.L. Landen *et al.*, Phys. Plasmas **17**, 056301 (2010).
[11] O.L. Landen *et al.*, to be published in Phys. Plasmas.
[12] S.W. Haan *et al.*, to be published in Phys. Plasmas.
[13] D.S. Clark *et al.*, Phys. Plasmas **17**, 052703 (2010).
[14] S.W. Haan *et al.*, Phys. Plasmas **12**, 056316 (2005).
[15] T.C. Sangster *et al.*, Phys. Plasmas **14**, 058101 (2007).
[16] D.C. Wilson *et al.*, Phys. Plasmas **5**, 1953 (1998).
[17] T.R. Dittrich *et al.*, Phys. Plasmas **6**, 2164 (1999).
[18] D.A. Callahan *et al.*, Phys.: Conf. Ser. **112**, 022021 (2008).
[19] A. Nikroo *et al.*, Phys. Plasmas **13**, 056302 (2006).
[20] K.C. Chen *et al.*, Fusion Sci. Technol. **49**, 750 (2006).
[21] J. Biener *et al.*, Fusion Sci. Technol. **49**, 737 (2006).
[22] G. Zimmerman and W. Kruer, Comments Plasma Phys. Controlled Fusion **2**, 51 (1975)
[23] M.M. Marinak *et al.*, Phys. Plasmas **8**, 2275 (2001).
[24] See National Technical Information Service Document No. UCRL 52276 (W.A. Lokke and W.H. Grosberger, Report No. UCRL 52276, 1977).
[25] A. Djaoui and S. Rose, J. Phys. B **25**, 2745 (1992).
[26] R. More *et al.*, Phys. Fluids **31**, 3059 (1988).
[27] J. Kilkenny *et al.*, Rev. Sci. Intrum. **66**, 288 (1995).
[28] R.J. Leeper *et al.*, Rev. Sci. Instrum. **68**, 868 (1997).
[29] T.J. Murphy *et al.*, Rev. Sci. Instrum. **72**, 773 (2001).
[30] V. Yu Glebov *et al.*, Rev. Sci. Instrum. **77**, 10E715 (2006).
[31] M. Landon *et al.*, Rev. Sci. Instrum. **72**, 698 (2001).
[32] S. Regan *et al.*, Phys. Plasmas **6**, 2072 (1999).
[33] P. Neumayer *et al.*, Rev. Sci. Instrum. **79**, 10F548 (2008).
[34] E.L. Dewald *et al.*, Rev. Sci. Instrum. **75**, 3759 (2004).
[35] E.L. Dewald *et al.*, Phys. Plasmas **13**, 056315 (2006).
[36] J. Kline *et al.*, Rev. Sci. Instrum. **81**, 10E321 (2010).
[37] J. McDonald *et al.*, Phys. Plasmas **13**, 032703 (2006).
[38] J.A. Oertel *et al.*, Rev. Sci. Instrum. **77**, 10E308 (2006).
[39] R.A. Lerche *et al.*, Rev. Sci. Instrum. **81**, 10D319 (2010).
[40] C.K. Li *et al.*, Phys. Plasmas **10**, 1919 (2003).
[41] M.D. Wilke *et al.*, Rev. Sci. Instrum. **79**, 10E529 (2008).
[42] J.A. Frenje *et al.*, Rev. Sci. Instrum. **72**, 854 (2001).
[43] J.A. Frenje *et al.*, Rev. Sci. Instrum. **79**, 10E502 (2008).
[44] J.A. Frenje *et al.*, Phys. Plasmas **17**, 056311 (2010).
[45] H.W. Herrmann *et al.*, Rev. Sci. Instrum. **79**, 10E531 (2008).
[46] H.W. Herrmann *et al.*, Rev. Sci. Instrum. **81**, 10D333 (2010).
[47] C.K. Li *et al.*, Phys. Rev. Lett. **100**, 225001 (2008).
[48] C.K. Li *et al.*, Phys. Rev. Lett. **102**, 205001 (2009).
[49] R.D. Petrasso *et al.*, Phys. Rev. Lett. **103**, 085001 (2009).
[50] R.E. Olson *et al.*, Phys. Rev. Lett. **91**, 235002 (2003).
[51] R.E. Olson *et al.*, Phys. Plasmas **11**, 2778 (2004).
[52] R.E. Olson *et al.*, Journal of Physics: Conference Series **244**, 032057 (2010).
[53] T.R. Boehly *et al.*, Phys. Plasmas **16**, 056302 (2009).
[54] H.F. Robey *et al.*, Phys. Plasmas **17**, 012703 (2010).
[55] R.E. Olson *et al.*, Rev. Sci. Instrum. **79**, 10E913 (2008).
[56] D.G. Hicks *et al.*, Rev. Sci. Instrum. **81**, 10E304 (2010).
[57] M.J. Edwards *et al.*, to be published in Phys. Plasmas.